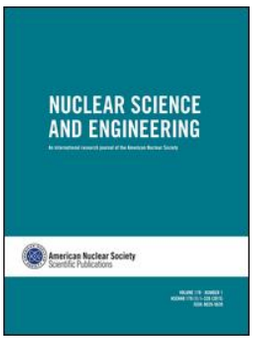

Nuclear Science and Engineering

ISSN: 0029-5639 (Print) 1943-748X (Online) Journal homepage: https://ans.tandfonline.com/loi/unse20

Measured and Calculated Rates of Decay Heat in Irradiated ^{235}U, ^{233}U, 239Pu, and ^{232}Th

S. B. Gunst, D. E. Conway & J. C. Connor

To cite this article: S. B. Gunst, D. E. Conway & J. C. Connor (1975) Measured and Calculated Rates of Decay Heat in Irradiated ^{235}U, ^{233}U, 239Pu, and ^{232}Th, Nuclear Science and Engineering, 56:3, 241-262, DOI: 10.13182/NSE75-A26738

To link to this article: https://doi.org/10.13182/NSE75-A26738

Published online: 12 May 2017.

NUCLEAR SCIENCE AND ENGINEERING: 56, 241-262 (1975)

Measured and Calculated Rates of Decay Heat in Irradiated ^{235}U, ^{233}U, ^{239}Pu, and ^{232}Th

S. B. Gunst, D. E. Conway, and J. C. Connor

Bettis Atomic Power Laboratory, Westinghouse Electric Corporation
West Mifflin, Pennsylvania 15122

Received May 9, 1974
Revised October 22, 1974

Samples of ^{235}U, ^{233}U, ^{239}Pu, and ^{232}Th have been irradiated in high neutron fluxes [$>10^{14}$ n/(cm^2 sec)] and their decay heat has been measured as a function of cooling time ranging from 14 to 4500 h after removal from the high flux. To measure the rate of heat emission, an underwater calorimeter has been developed. For the measured exposure histories, decay heat has also been calculated for concentrations of 190 fission products, all significant heavy isotopes, and structural nuclides. Account is taken of the energy carried by gamma rays that escape the calorimeter. Measurements and calculations of the decay heat captured within the calorimeter agree within two standard deviations for all samples and cooling times and, in general, agree within 2%. For the ^{235}U sample, calculations based on the Proposed ANS Standard ANS-5.1 (ANSI N18.6) agree with the measurements within a few percent.

I. INTRODUCTION

Decay heat in irradiated nuclear fuel is an important factor in establishing the maximum power for an operating reactor. This is true because it is necessary to limit fuel and cladding temperatures to safe margins following reactor shutdown, particularly after a loss-of-coolant accident. For emergency core cooling systems or residual heat removal systems, decay-heat information is particularly important immediately after reactor shutdown and during the first day following. However, decay heat remains important hundreds or thousands of hours after shutdown because of its presence during reactor refueling and during the storage, shipment, or reprocessing of spent fuel. Heat from beta- and gamma-ray decay of fission products under equilibrium conditions in an operating reactor produces from 5 to 10% of the power and affects the power distribution over the core. Information on decay heat is thus important for both the nuclear and the thermal-hydraulic design of nuclear reactors.

In addition to the purposes noted, information on decay heat is important for irradiation and reactivity experiments to account for the reactivity perturbation introduced by decay heat in irradiated fuel samples.

Although many investigators have published information on decay heat calculations or evaluations,[1-6] experimental measurements of decay

[1]T. R. ENGLAND, "An Investigation of Fission Product Behavior and Decay Heating in Nuclear Reactors," PhD Thesis, University of Wisconsin (1969).

[2]K. SHURE, "U^{235} Fission Product Decay Energy 1972 Re-Evaluation," WAPD-TM-1119, Bettis Atomic Power Laboratory (1972).

[3]A. M. PERRY, F. C. MAIENSCHEIN, and D. R. VONDY, "Fission-Product After Heat—A Review of Experiments Pertinent to the Thermal-Neutron Fission of ^{235}U," ORNL-TM-4197, Oak Ridge National Laboratory (1973).

[4]M. LOTT, "Residual Power Due to Fission Products," IAEA Review Paper No. 15, in "Fission Product Nuclear Data," IAEA Panel on Fission Product Nuclear Data, Bologna, Italy (Nov. 1973).

[5]A. TOBIAS, *J. Nucl. Energy*, **27**, 725 (1973).

[6]L. COSTA and R. deTOURREIL, *J. Nucl. Energy*, **25**, 285 (1971).

heat have been very limited,[7-11] especially for conditions typical of operating reactors and for different nuclear fuels. For the most part, estimations of decay heat for conditions of interest have been based on the application and extrapolation of available ^{235}U data. (Consistent with common usage, the term "decay heat" is used in this paper for the rate of energy release by radioactive decay.)

In this report, calorimetric investigations are described for the integral measurement of rates of decay heat in samples of ^{235}U, ^{233}U, ^{239}Pu, and ^{232}Th irradiated with high fluxes and for exposures representative of those achieved in a power reactor. Calorimetric measurements were started as soon as possible after irradiation—about 14 h after reactor shutdown—and continued for ~4500 h.

To implement decay heat measurements, an underwater calorimeter for highly radioactive samples has been developed. Adequate shielding of personnel is provided by operating the calorimeter under eight or more feet of water. Decay heat is determined by measuring the temperature as a function of time for the volume of water inside the calorimeter following insertion of the irradiated sample. Compared to earlier investigations of decay heat under this program,[11] the calorimeter developed for the experiments described here is similar in design but has significantly improved features.

II. DESIGN OF SAMPLES AND CALORIMETER

The irradiation samples (Fig. 1) for the decay heat experiments are four-rod assemblies of

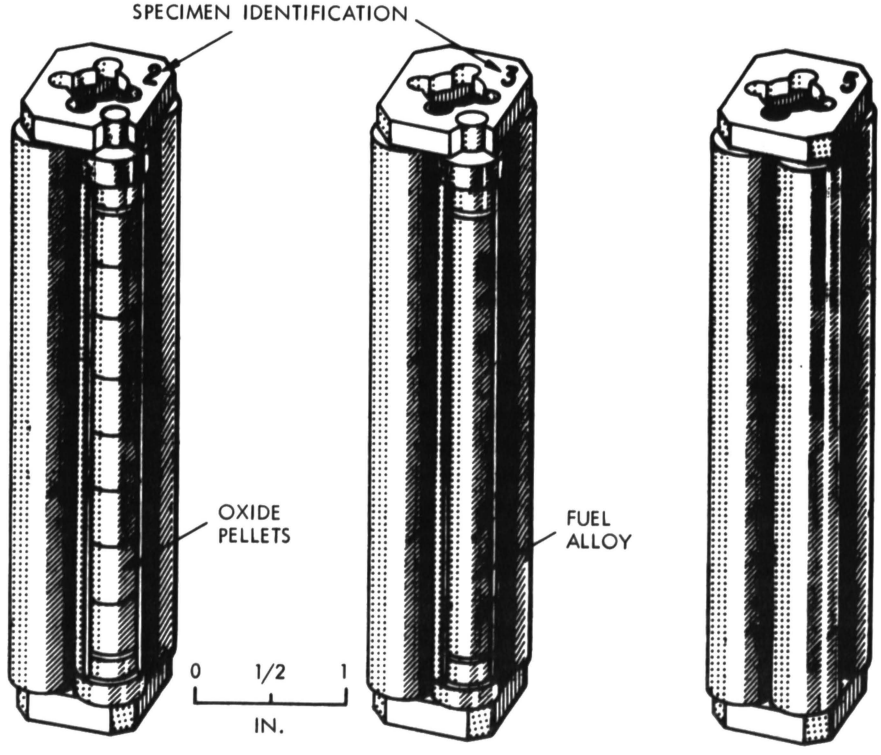

Fig. 1. Samples of four-rod geometry showing oxide pellets, alloy bars, and Zircaloy-2 cladding consisting of tubes, end caps, and tube sheets.

[7]Available experimental results by D. L. HILL and L. LANZL; R. A. DAY and C. V. CANNON; L. BORST, E. L. BRADY, and A. TURKEVICH; and N. SUGARMAN et al. are discussed and referenced in K. WAY and E. P. WIGNER, *Phys. Rev.*, **73**, 1318 (1948); and in Ref. 8.

[8]J. F. PERKINS and R. W. KING, *Nucl. Sci. Eng.*, **3**, 726 (1958).

[9]M. LOTT, G. LHIAUBET, F. DUFRECHE, C. DEVILLERS, and R. deTOURREIL, "Calorimetric Measurement of the Energy Released by ^{235}U Fission Products for Cooling Times Between 70 Sec and 7×10^6 Sec," AEC-tr-7472, Translation of Paper No. 28/73 Spe, Commissariat a l'Energie Atomique, Fontenay-aux-Roses, France (1973).

[10]C. DEVILLERS, G. LHIAUBET, M. LOTT, VAN DAT N'GUYEN, and F. DUFRECHE, "Calorimetric Measurement of Residual Power of Rapsodie and Fortissimo Fuel Elements," AEC-tr-7479, Translation of Paper No. 29/73 Spe, Commissariat a l'Energie Atomique, Fontenay-aux-Roses, France (1973).

[11]J. J. SCOVILLE, "Fission Product Decay Heat," MS Thesis, University of Pittsburgh (1959).

Zircaloy-2 clad metal-alloy bars or sintered oxide pellets. In addition to fuel materials, the samples contain structural materials comprising the nonfuel components of the alloy bars or oxide pellets and the cladding tubes, end caps, and tube sheets. The initial or pre-irradiation constituents of the four irradiation samples of interest are given in Table I. As described in Ref. 12, the samples were irradiated along with cobalt flux-monitor wires—four peripheral bare monitors and an axial train with cadmium-covered end sections.

As shown in the cutaway view of Fig. 2, the underwater calorimeter is a vacuum bottle with the space (1,2) between concentric cylinders (3,4) evacuated through the hose (5) when the calorimeter is in use. To minimize heat loss, the opposing surfaces are silvered. A stainless-steel plate for the calorimeter top (6) has an attached concave thermal insulator of Teflon (7) on its inner side.

TABLE I

Initial Constituents of the Irradiated Samples

	^{235}U Sample 25	^{233}U Sample 45	^{239}Pu Sample 19	^{232}Th Sample 41
^{232}Th[a]				149.7973
^{232}U		0.00007		
^{233}U		1.3714		
^{234}U	0.0184	0.0325		
^{235}U	1.7074	0.0028		
^{236}U	0.0048	0.0003		
^{238}U	0.1023	0.0051		
^{239}Pu			1.0406	
^{240}Pu			0.0675	
^{241}Pu			0.0054	
^{242}Pu			0.0002	
C	0.7288			
Zr	212.4788	92.2757	93.4534	92.0546
Hf	0.0130	0.0067	0.0067	0.0066
Al		50.7059	50.2074	
O				20.6593
Sample Volume (ml)	33.5513	33.6449	33.7886	33.6571

[a]The masses are expressed in grams.

[12]S. B. GUNST, J. C. CONNOR, and D. E. CONWAY, "Measurements and Calculations of Heavy Isotopes in Irradiated Fuels and of ^{233}U Fission-Product Poisoning," WAPD-TM-1182, Bettis Atomic Power Laboratory (1974).

Passing through the top are a tapered port (8) for admitting a sample, a feed-through Nylon shaft (9) for coupling a motor-driven shaft (10) to a stirrer shaft (11), and a thermopile (12,13,14) consisting of four series-connected Chromel-Alumel thermocouples with successive junctions on alternate sides of the top. The thermopile is used with a highly sensitive recording potentiometer to measure the temperature difference between the water inside the calorimeter and the canal water outside the calorimeter. The thermocouple jackets consist of thin-walled stainless-steel tubes (12) that carry the thermocouple wires from hot junctions inside the calorimeter to cold junctions in the cap (14). Since the cap is essentially surrounded by canal water, the cold junctions remain at the temperature of the canal water, routinely controlled to ±0.003C°.

A Teflon gasket (15) and a rubber O-ring (16) prevent flow of water between the inside and outside of the calorimeter. A perforated stainless-steel basket (17) attached at the top port supports a sample during calorimetric measurement. Two four-bladed propellers at different elevations on the stirrer shaft (11) are driven at 288 r/min by a long shaft (10) coupled to an electric motor (18) above the surface of the water. During measurements, the calorimeter is supported on a working tray ≥8 ft below the surface in the canal of the Advanced Reactivity Measurement Facility (ARMF-I).

During calorimeter operation, the stirrer maintains an essentially uniform temperature throughout the water volume inside the calorimeter at any instant. As shown in Fig. 3, a tapered "plug" with an O-ring seal is used to close the tapered port during calorimetric measurements. A long handle attached to the tapered plug facilitates moving the plug from above the canal water surface.

To flush the calorimeter following a measurement and the removal of the sample, the tapered plug is replaced by a purge tube of similar geometry (19 in Fig. 2) where the handle is now a tube through which canal water can be pumped into the calorimeter. As shown in Fig. 3, the plug of the purge tube contains axial channels along its tapered surface to permit the discharge of water from the calorimeter.

Figure 3 also shows a third item of similar geometry to the long-handled tapered plug but with an electrical heater of the four-rod sample geometry attached to the bottom end. The power lines pass through the handle to the surface. When installed, the heater occupies the same space as a sample inside the calorimeter and is used to calibrate the calorimeter over the range of interest (0 to 50 W).

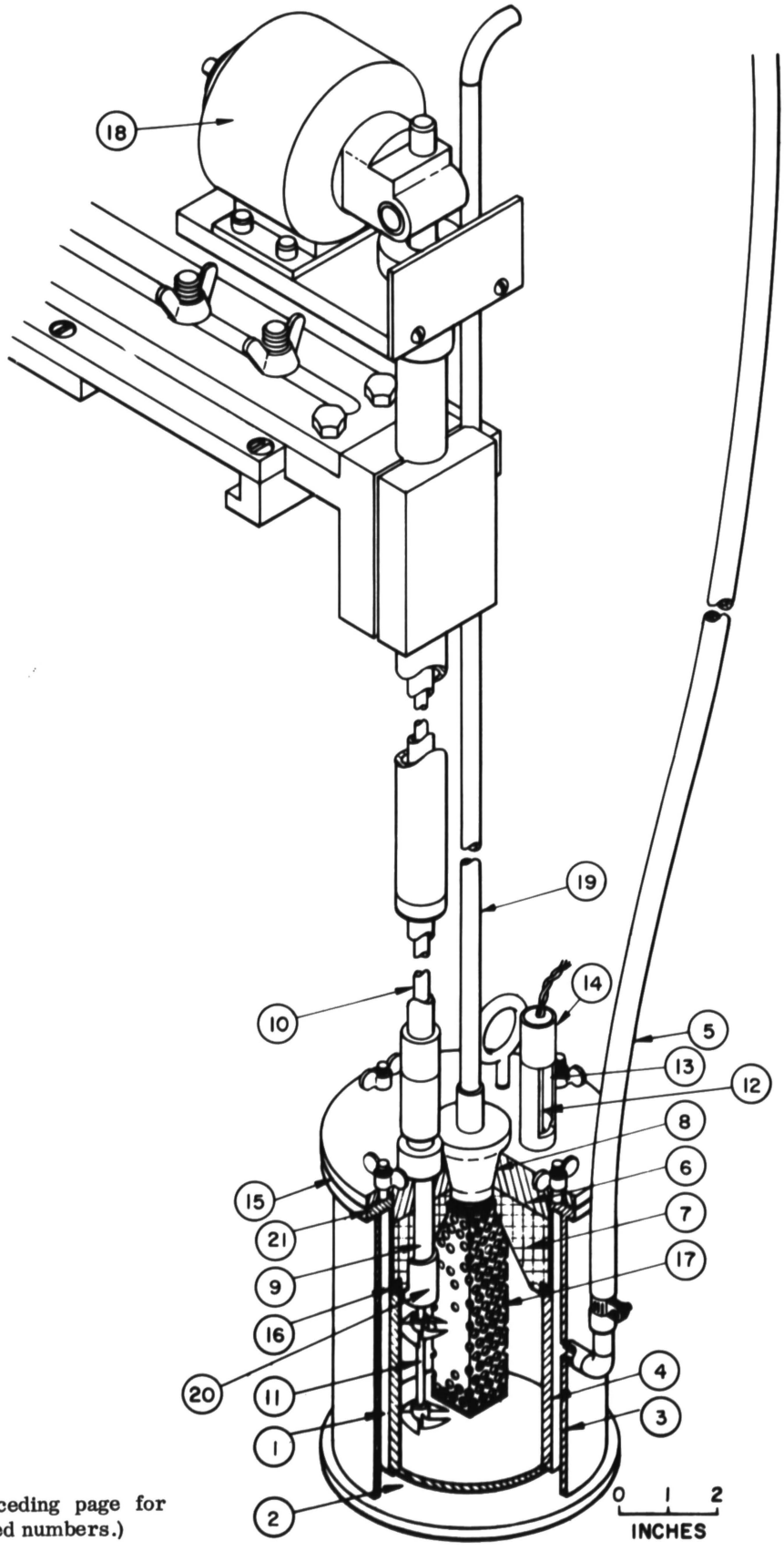

(Refer to the preceding page for definitions of circled numbers.)

Fig. 2. Sectional view of underwater calorimeter.

III. EXPERIMENTAL METHODS

III. A. General Treatment

To operate the calorimeter, first the water inside the calorimeter is flushed to bring the calorimeter to ambient canal water temperature. Then, with the stirrer running, a heat dissipating sample or heater (in thermal equilibrium with canal water) is moved from the water outside to that inside the calorimeter. It is inserted into the perforated basket at time zero and the sample port is plugged immediately. The time dependence of the temperature of the water inside the calorimeter is a function of the rate of heat dissipation within the calorimeter. The typical recording potentiometer trace given in Fig. 4 illustrates the fact that the increase in temperature is almost linear with time because the thermal leakage out of the calorimeter is small.

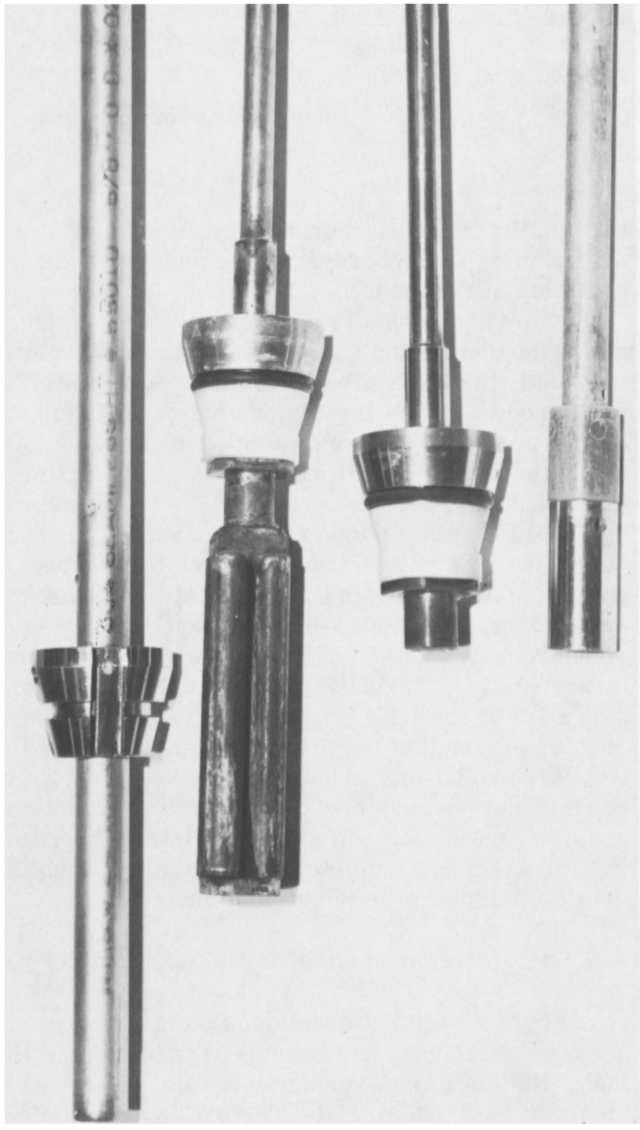

Fig. 3. Bottom end of long-shaft items. Left to right are: purge tube with channel for water discharge, four-rod electrical heater for calibrating calorimeter, plug for tapered port, drive shaft for coupling to male hexagonal end of stirrer.

At the end of a measurement, the sample (or heater) is removed from the calorimeter, the purge tube is inserted, and the water purge pump is turned on. Although the water temperature difference detected by the thermopile quickly returns to near zero, flushing is continued for 2 min to ensure that the walls and other components of the calorimeter are cooled before undertaking the next measurement.

If the rate of heat absorbed inside the calorimeter due to the heater or sample is given by q and the small amount of heating due to the stirrer is q_s, the temperature difference $\theta(t)$ between the water inside and the water outside the calorimeter is a function of time t and changes at the rate $\dot{\theta}(t)$. As previously mentioned, the water outside the calorimeter in the canal provides a reference temperature constant within 0.003C°. To first order, $\dot{\theta}(t)$ is proportional to $(q + q_s)$. However, $\dot{\theta}(t)$ is not constant with time because of heat loss from the calorimeter. At any instant, the heat loss is proportional to $\theta(t)$, and the total heating in the calorimeter is given by

$$q + q_s = A\,\theta(t) + B\dot{\theta}(t) \quad , \tag{1}$$

where A and B are constants. The value of A depends on the thermal leakage through the inner walls and surfaces of the calorimeter. The value of B depends on the thermal capacities of the water, of the inner wall of the calorimeter, and of various other components inside the calorimeter. Calibration of the calorimeter involves the determination of q_s, A, and B while measurements of the heating q due to an arbitrary sample involves the solution of Eq. (1) for q.

III. B. Calibration of Calorimeter

Values of the calibration constants q_s, A, and B are determined by running three types of tests designed to emphasize each of the constants:

1. With the stirrer running and no heat applied to the electrical heater, the calorimeter is operated overnight until a constant temperature is reached within the calorimeter. Under these conditions, q_s is emphasized and q and $\dot{\theta}$ are zero.
2. By applying excessive heating and then decreasing it, the calorimeter is operated by essentially balancing the rate of heat loss against the input rate for several heater

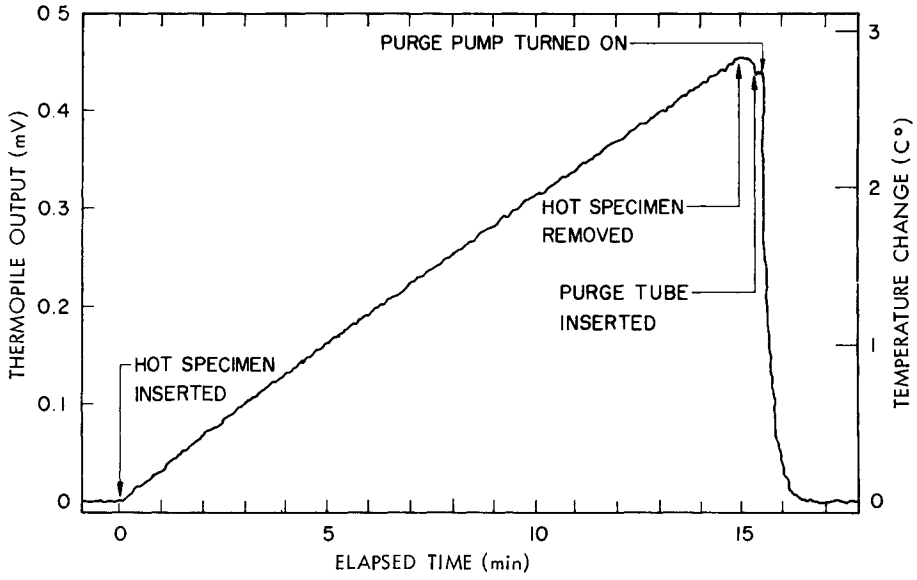

Fig. 4. Typical response of recording potentiometer to a 30-W heat source within underwater calorimeter. Scales on both axes are adjustable by switch settings.

wattages, q. For such conditions, the temperature approaches equilibrium and the $B\dot{\theta}$ and q_s terms contribute only a few percent in Eq. (1).

3. Data as illustrated in Fig. 4 are obtained for heater wattages q of 10 to 50 W. Under the conditions indicated, the $B\dot{\theta}$ term in Eq. (1) is at least an order of magnitude larger than the $A\theta$ and q_s terms.

To obtain good statistics in evaluating the three constants, several tests as indicated in type 1 have been run, about a dozen tests of type 2 and about 50 runs of type 3. Moreover, the data from type 3 runs are processed in such a way as to provide from five to eight tests per run. In doing so, the data are processed the same as data obtained with an irradiated sample in the calorimeter. Each curve is divided into from seven to ten equal time increments. The first two increments are discarded to make sure that the water-convection pattern is established and that the temperature distribution within the calorimeter has achieved a so-called dynamic "equilibrium" following insertion of the hot specimen. Each curve segment retained is analyzed by evaluating $\dot{\theta}$ for each segment from the change of θ over the segment and the length of the time increment. Here θ is the average value over the segment and q is the rate of heat dissipation of the hot specimen. With approximate values for the constants q_s and A determined as indicated, the constant B is evaluated for each segment and averaged to provide a value for each curve. The rms deviation of all the values of B per curve is used to check the quality of each curve. Typically, the rms deviation is of the order of 4% and the standard deviation of the mean is $< 2\%$.

Calibration measurements have been obtained at the beginning and end of every period of operation and thus have been interspersed with the measurements of irradiated samples over the entire period of the sample measurements. This not only provides additional data for the calibration constants, but also serves to check the reproducibility of the measurement system at each period of operation. Operation of the recording potentiometer has also been routinely checked every operating period by measuring a series of standard voltages. The final values of q_s, A, and B are 0.054 ± 0.020 W, 0.50 ± 0.05 W/C°, and 81.8 ± 1.6 W min/C°, respectively, and comprise a consistent set that best fits all the data. Here the standard deviations are based on the precision of reading curves and are increased to account for possible systematic effects associated with reading the precision ammeter and voltmeter to obtain the power input to the electrical heater.

III. C. Measurement of Irradiated Samples

To obtain substantial fissions and fission-product concentrations, fuel-sample irradiations at the Idaho National Engineering Laboratory were carried out in the Materials Testing Reactor (MTR) until its shutdown and subsequently in the Advanced Test Reactor (ATR), where the thermal-neutron flux is 3 to $5 \times 10^{14}/(\text{cm}^2\ \text{sec})$. Following the final irradiation cycle, the samples were discharged from the ATR as expeditiously as possi-

ble and transferred to the canal of the Advanced Reactivity Measurement Facility where calorimetric measurements were carried out.

Analysis of irradiated sample calorimetric data is similar to the analysis of type 3 data. Each curve is divided into approximately ten increments and all but the first two are analyzed per Eq. (1) to obtain q. An average value for q with its measurement precision is determined for each curve.

Contributors to the standard deviation of the measured value of q are given in Table II for various heat rates. Values in the table are the contributions to the standard deviation of q in watts.

IV. CALCULATIONAL METHODS

The experiments described are important for checking calculations of decay heat. To compare calculations with measurements is rather involved and requires an understanding of the various sources of decay heat as well as accounting for the probability that any given heat component will be captured inside the calorimeter. To calculate the decay heat emitted by an irradiated sample, the initial constituents of the sample (Table I) and its complete exposure history are taken into account. As described in Ref. 12, the exposure history combines bare and cadmium-covered cobalt monitor data, obtained every cycle, with nickel activation data and with daily power logs for the irradiation facility. The resulting detailed three-group exposure history is presented for each sample in Ref. 13, and a summary of the integrated exposures appears in Table III. By means of a procedure called COMBO, concentrations of heavy isotopes, fission products and structural nuclides, together with the accumulated fissions and fission rates, are computed as functions of irradiation. Following irradiation, the rates of decay and the rates of energy emission by decaying heavy isotopes, structural nuclides, and all the fission products are computed as functions of cooling time (time after irradiation). In all COMBO calculations including those for fission products, both decay and capture are taken into account in explicit nuclide-by-nuclide calculations using methods and data presented in Ref. 12.

Postirradiation concentrations calculated for the detailed exposure history of each sample have

[13]S. B. GUNST, D. E. CONWAY, and J. C. CONNOR, "Decay Heating Measurements and Calculations for Irradiated ^{235}U, ^{233}U, ^{239}Pu, and ^{232}Th," WAPD-TM-1183, Bettis Atomic Power Laboratory (1974).

TABLE II

Uncertainty Contributions to the Measurement of Heat Rate
(All values are in watts)

Source of Uncertainty	q								
	50	40	30	20	10	5	2	0.5	0.2
Measurement of $\theta(t)$	1.0	0.8	0.6	0.4	0.2	0.14	0.09	0.05	0.03
A	0.15	0.12	0.09	0.06	0.04	0.02	0.02	0.008	0.008
B	1.0	0.8	0.6	0.4	0.2	0.10	0.04	0.010	0.004
q_s	0.03	0.03	0.03	0.03	0.03	0.03	0.03	0.03	0.03
Overall δq	1.42	1.14	0.85	0.57	0.29	0.18	0.10	0.060	0.043
$(\delta q/q)$ (%)	3	3	3	3	3	4	5	12	22

TABLE III

Summary of Irradiations for Samples

Fuel Material	Sample	Irradiation Time (3-week cycles)	Flux Ratio Epithermal/Thermal $(\varphi_1 + \varphi_2)/\varphi_3$	Integrated $\varphi_3 t$ 10^{21} n/cm^2	Fission Density 10^{20} fission/ml	% Depletion[a]
^{235}U in Zr	25	4	2.16	1.04	0.92	47
^{233}U in Al	45	5	1.87	1.28	0.89	52
^{239}Pu in Al	19	4	2.34	1.14	0.79	76
Natural ThO_2	41	1	3.98	0.52	0.03	0.51

[a]For Samples 25, 45, 19, and 41, % depletion refers to the change from the initial concentration of ^{235}U, ^{233}U, ^{239}Pu, and ^{232}Th, respectively.

been compared with postirradiation mass measurements for total and isotopic uranium, total and isotopic plutonium, ^{137}Cs, and the neodymium isotopes. As shown in Ref. 12, these measured and calculated results agree remarkably well—generally within 1 wt%. Such agreement confirms the adequacy of the calculations of concentrations, fissions, fission rates, and rates of decay in the irradiation samples of interest.

IV. A. The Gamma-Ray Spectrum

Since the absorption of gamma rays depends on their energy, a means of describing the gamma-ray spectrum is needed. To do so, a group structure common in the literature[8,14-17] is adopted as shown in Table IV. The gamma-ray spectrum for all decaying heavy isotopes, activated structural nuclides, and gross fission products is described by assigning the appropriate fraction of the gamma-ray energy to each of the eight groups given in Table IV.

TABLE IV

Energy Groups Used to Describe Gamma-Ray Spectra

Group	Energy Range (MeV)	Average Energy (MeV)
0	0 - 0.1	0.07
1	0.1 - 0.4	0.3
2	0.4 - 0.9	0.63
3	0.9 - 1.35	1.10
4	1.35 - 1.8	1.55
5	1.8 - 2.2	1.99
6	2.2 - 2.6	2.38
7	>2.6	3.1

IV. B. Sources of Heat

IV.B.1. Heavy Isotopes

All the significant heavy isotopes and their couplings by neutron capture (n,γ) and n, $2n$ reactions, or by beta-particle decay (β^-), alpha-particle decay (α), or electron capture (ϵ) are shown in Fig. 5. Although not indicated in Fig. 5, fission in any of the isotopes produces fission products according to yield probabilities. In the calculations, all nuclides in Fig. 5 are permitted to decay and to capture and fission according to their capture and fission cross sections. If particular decay or capture reactions are not indicated in the figure, the resulting product is insignificant.

For the heavy isotopes shown in Fig. 5, energies per decay are incorporated in the heating calculations for nine of the isotopes as shown in

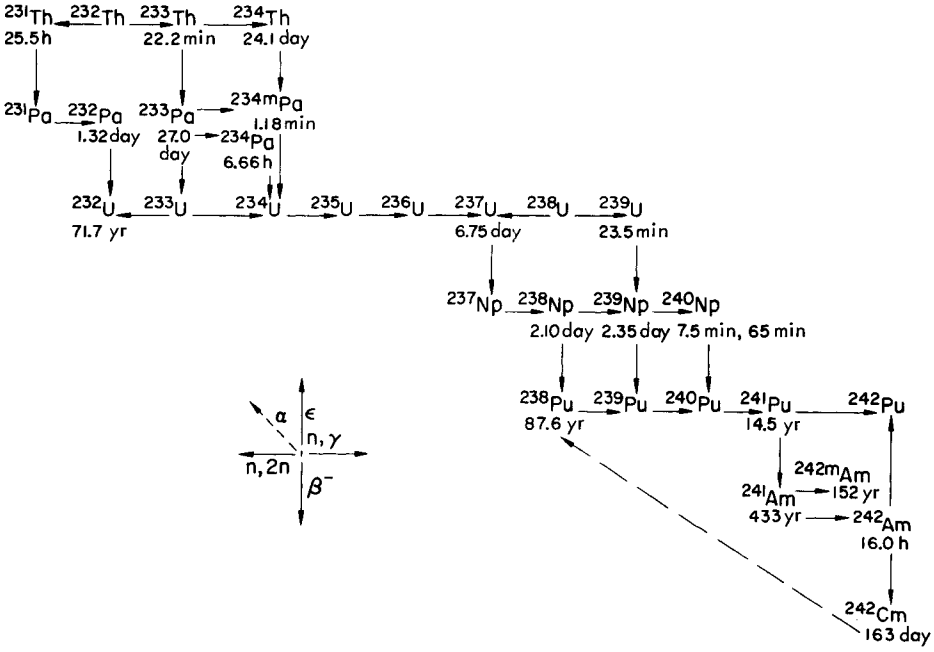

Fig. 5. Significant heavy isotopes and how they are coupled.

[14]J. MOTEFF, "Fission Product Decay Gamma Energy Spectrum," APEX-134, Aircraft Nuclear Propulsion Project, General Electric Company (1953).

[15]F. H. CLARK, "Decay of Fission Product Gammas," NDA-27-39, Nuclear Development Associates, Inc. (1954).

[16]W. E. KNABE and G. E. PUTNAM, "The Activity of the Fission Products of U^{235}," APEX-448, Internuclear Company, Inc. for Aircraft Nuclear Propulsion Department, General Electric Company (1958).

[17]K. SHURE, "Fission Product Decay Energy," WAPD-BT-24, 1-17, Bettis Atomic Power Laboratory (1961).

Table V. The nine isotopes selected are more than sufficient to ensure accounting for heavy-isotope decay heat for the fuels and cooling times of interest in the period from 10 to 10^4 h after irradiation. In other cases, particularly at earlier cooling times, additional nuclides are important heat contributors.

Because of the loss of energy carried by neutrinos in beta-particle decay, the end-point energy for a given beta-particle transition as given in the *Nuclear Data Sheets* is multiplied by the ratio $E_\beta^{av}/E_\beta^{max}$ derived from published information[18] and data[19] and calculated by Goldsmith and Shure at the authors' Laboratory. The result given in Table V is the average energy carried by the beta particles themselves and represents the contribution to the heat by beta-particle transitions in a given nuclide.

For gamma-ray transitions, it is important to account for internal conversion explicitly because a conversion electron loses energy in the calorimeter like a beta particle rather than like a gamma ray. The binding energy required to remove a conversion electron from its orbit in an atom is included with the conversion-electron energy given in Table V. This is reasonable because the x rays produced as the atom returns to its neutral state following internal conversion are sufficiently soft so that they have a high probability for capture within the calorimeter along with the conversion electron. Internal conversion is more important in heavy isotopes than it is in fission products or structural isotopes because it is high when the atomic number is high. It is also high when the transition energy is low. Most low energy gamma-ray transitions lose their energy within the calorimeter whether or not they produce conversion electrons. Accounting for internal conversion for calorimetric measurements is important primarily for the heavy isotopes and for particular fuels such as irradiated ^{232}Th and ^{238}U.

In Table V the sum of the alpha-particle, beta-particle, and conversion-electron energies per decay gives the total charged particle heat per decay that is absorbed in or very near the irradiation sample. In contrast, the probability for the absorption of gamma rays depends on the energy of the particular gamma ray of interest. The gamma-ray spectrum, therefore, is important and is given for each decaying heavy isotope in the last eight columns of Table V as the percent of the gamma-ray energy in each of the eight gamma-ray energy regions adopted as described in Sec. IV. A.

IV.B.2. Fission Products

Concentrations and decay heat of 190 fission products in 80 cross-coupled linear chains are computed by the COMBO procedure as functions of the exposure history including cooling time or time at zero flux. The step-by-step exposure histories in three energy groups are tabulated in Ref. 4; the calculational methods, chain descriptions, cross sections, yields, and other pertinent data are given in Ref. 12. Compared to the 352 fission products commonly used in the decay-heat calculations of the CINDER program,[1] the 190

[18] R. D. EVANS, *The Atomic Nucleus*, p. 619, McGraw-Hill Book Company, Inc., New York (1955).

[19] M. E. ROSE, N. M. DISMUKE, C. L. PERRY, and P. R. BELL, "Tables of Fermi Functions," Appendix II in *Beta- and Gamma-Ray Spectroscopy*, K. SIEGBAHN, Ed., Interscience Publishers, Inc., New York (1955).

TABLE V

Energy per Decay Associated with Charged Particles and Gamma Rays in Decaying Heavy Isotopes and Spectral Distribution of the Gamma-Ray Energy

Nuclide	Half-Life	Decay Energy (MeV)				Gamma Spectrum (% of Gamma-Ray Energy in Group Indicated)							
		Alpha	Beta	Conversion Electron	Gamma-Ray	0	1	2	3	4	5	6	7
^{233}Pa	27.0 day	0	0.0636	0.1778	0.1718	1.58	94.37	4.05	0	0	0	0	0
^{234}Th[a]	24.1 day	0	0.8762	0.0253	0.0212	46.78	4.68	12.82	29.10	3.04	3.58	0	0
^{234}Pa	6.66 h	0	0.1749	0.3439	1.5710	0.16	7.24	52.73	33.63	6.24	0	0	0
^{237}U	6.75 day	0	0.0656	0.1942	0.0854	27.99	72.01	0	0	0	0	0	0
^{238}Pu	87.6 yr	5.4860	0	0	0	---	---	---	---	---	---	---	---
^{239}Np	2.345 day	0	0.1093	0.2165	0.1169	0.00	99.88	0.12	0	0	0	0	0
^{241}Pu	14.5 yr	0	0.0208	0	0	---	---	---	---	---	---	---	---
^{241}Am	432.7 yr	5.4944	0	0.0408	0.0217	100.00	0	0	0	0	0	0	0
^{242}Cm	163.0 day	6.1006	0	0.0104	0	---	---	---	---	---	---	---	---

[a] Includes 1.177-min ^{234m}Pa.

fission products selected for the COMBO procedure do a comparable job of describing decay heat at times of interest for the calorimetric measurements of this report. Results of COMBO with 190 fission products and CINDER with 352 fission products have been compared for typical cases of irradiated ^{235}U and ^{233}U and agree within a few percent for all cooling times after 4 h and within 1% in many of the cases.

The beta- and gamma-ray energies per decay and group cross sections incorporated in the COMBO library[12] are based on the library for fission products prepared for the CINDER program.[1] These data are based on the nuclide library of Ref. 20 and include revisions by England in 1970, data changes suggested by Shure[2] in 1972, and additional changes by the authors in 1973.

As mentioned for heavy isotopes, the spectrum of gamma rays for accumulated fission products is important and has been calculated for the sample of irradiated ^{235}U by Shure and Wallace at the authors' Laboratory. The resulting spectra in terms of the groups described in Table IV are given in Table VI and are based on the work of Perkins and King[8] as extended by Koebberling et al. (see discussion in Ref. 2) and Battat et al.[21] and with updated data used by Shure[2] in a procedure called FSTAB. For each of 21 different cooling times, the percent of the gamma-ray energy in each of eight energy groups is shown in Table VI where the horizontal sum at each cooling time totals 100%.

IV.B.3. Structural Nuclides

In the Zircaloy-2 cladding of all samples and in the zirconium component of the ^{235}U-alloy sample, activations that contribute to decay heat are shown in Fig. 6. The naturally occurring nuclides ^{94}Zr and ^{96}Zr have abundances of 17.4 and 2.8%, respectively, and produce the capture and decay products indicated. In the beta-particle decay of ^{95}Zr, only 0.6% of the gamma rays and 0.19% of the gamma-ray transition energy is associated with the 86.6-h metastable state ^{95m}Nb that decays to the ^{95}Nb ground state. With negligible error, therefore, the gamma-ray transition energy in ^{95m}Nb is assumed to be produced promptly, a procedure that permits excluding the ^{95m}Nb branch

[20]T. R. ENGLAND, "Time-Dependent Fission-Product Thermal and Resonance Absorption Cross Sections," WAPD-TM-333, Bettis Atomic Power Laboratory (1962) and Addendum No. 1 (1965).

[21]M. E. BATTAT, D. J. DUDZIAK, and H. R. HICKS, "Fission Product Energy Release and Inventory from ^{239}Pu Fast Fission," LA-3954, Los Alamos Scientific Laboratory (1968).

TABLE VI

Gamma-Ray Energy Spectra for Fission Products in Irradiated ^{235}U Sample 25 at Various Cooling Times (Energy groups are defined in Table IV)

Cooling Time (h)	Percent of Fission-Product Gamma-Ray Energy in Group Indicated							
	0	1	2	3	4	5	6	7
0.1	0.29	7.59	33.61	19.57	18.52	6.49	7.15	6.78
1	3.36	8.04	43.39	13.80	17.57	5.09	6.88	1.87
2	2.99	9.15	46.14	12.64	17.58	4.90	5.16	1.44
4	2.10	11.04	48.47	11.93	17.64	4.26	3.53	1.03
8	1.62	12.79	51.79	11.16	16.96	2.76	2.07	0.85
10	1.73	13.22	52.80	10.74	16.67	2.24	1.74	0.86
20	2.51	14.11	53.99	8.97	16.87	1.08	1.40	1.07
40	3.29	14.32	51.19	7.61	19.76	0.56	1.79	1.48
80	3.79	13.93	45.71	6.49	25.33	0.34	2.41	2.00
100	3.85	13.63	44.03	5.97	27.43	0.30	2.62	2.17
200	3.66	12.26	40.12	3.88	33.93	0.18	3.26	2.71
400	2.96	10.79	39.80	1.87	37.81	0.09	3.65	3.03
800	2.09	9.06	49.54	0.98	32.50	0.08	3.14	2.61
1 000	1.88	8.33	56.08	0.85	27.84	0.10	2.69	2.23
2 000	1.35	5.17	83.74	0.40	7.75	0.24	0.74	0.61
4 000	1.17	2.46	95.08	0.24	0.53	0.47	0.02	0.03
8 000	2.40	2.67	92.10	0.35	0.96	1.47	0.01	0.04
10 000	3.68	3.85	88.03	0.49	1.54	2.34	0.01	0.06
20 000	5.15	5.40	83.00	0.73	2.22	3.36	0.03	0.11
40 000	0.97	1.24	96.50	0.21	0.42	0.62	0.01	0.03
80 000	0.04	0.21	99.72	0.01	0.01	0.01	0.00	0.00

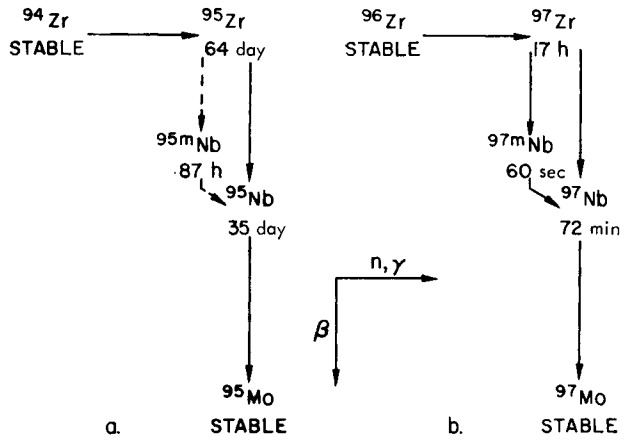

Fig. 6. Activation products in the irradiation of natural zirconium.

shown by dashed lines in Fig. 6a. As indicated in Fig. 6, it is found that ^{95}Zr, ^{95}Nb, ^{97}Zr, ^{97m}Nb, and ^{97}Nb are contributors to the decay heat in irradiated natural zirconium that should be taken into account.

Because of the geometry of the fuel rods and cladding of the four-rod sample, resonance integrals for neutron capture in ^{94}Zr and ^{96}Zr are self-shielded. Effective resonance cross sections for ^{94}Zr and ^{96}Zr, calculated using the ZUT program,[22] are 0.025 and 0.36 b, respectively, for the cladding, and 0.023 and 0.30 b, respectively, for the cladding plus alloy.

The zirconium isotopes ^{94}Zr and ^{96}Zr and their activation products shown in Fig. 6 are included among the nuclides in the 190 fission products of the COMBO library. To incorporate non-fuel activations in the cladding and alloy in calculations for an irradiated sample, the initial concentrations of ^{94}Zr and ^{96}Zr present in the cladding and fuel alloy for each irradiation sample are taken into account. The beta- and gamma-ray energies per decay for each of the activated zirconium nuclides and their decay products are included in the COMBO library as taken from the CINDER library and as described in Sec. IV. B. 2. The spectrum of gamma rays is given in Table VII for each of the zirconium activation products and is expressed as a percent of the gamma energy in each of the eight energy groups adopted as previously described.

IV. C. Deposition of Emitted Energy

Although the energy emission from an irradiated sample due to charged particles (beta and alpha particles and conversion electrons) is absorbed inside the calorimeter, only a fraction of the emitted gamma rays are so absorbed. To determine the fraction of gamma-ray heating absorbed inside the calorimeter, Monte Carlo calculations are carried out for the average energy of each of the eight gamma-ray energy groups described in Table IV.

To obtain reliable results, the geometry and constituents of all components in the sample-calorimeter-canal system must be described in substantial detail. Twenty components are specified as listed in Table VIII. To facilitate Monte Carlo calculations, the canal is described as a 10-in.-thick blanket of water outside the calorimeter and a surrounding black absorber.

For each of the group-average energies specified in Table IV, Monte Carlo calculations are carried out that give the probability that gamma rays having the specified average energy and uniformly distributed over the sample volume will be absorbed in each of the 20 components. Because the fuel material differs for different samples, Monte Carlo problems for each energy are run for each type of sample.

Results of the Monte Carlo calculations are presented in Table VIII for the sample of ^{235}U in zirconium, and show the percent of the gamma rays, of the energy specified by the group indicated in the heading, that are absorbed in each of the 20 components described. The components are listed in column 1 and cross referenced in column 2 to figure numbers with item numbers shown in parentheses. As indicated on the bottom line, the distribution among the components sums to 100% at each energy. Similar tables for the samples of ^{233}U or ^{239}Pu in aluminum and for the natural ThO_2 sample have also been prepared.

TABLE VII

Gamma-Ray Spectra for Zirconium Activation Products

Nuclide	Percent of Gamma-Ray Energy in Group Indicated							
	0	1	2	3	4	5	6	7
^{95}Zr	0	0.05	99.95	0	0	0	0	0
^{95}Nb	0	0	100.00	0	0	0	0	0
^{97}Zr	0	1.38	85.74	5.38	6.75	0.75	0	0
^{97m}Nb	0	0	100.00	0	0	0	0	0
^{97}Nb	0	0.03	97.36	2.26	0.35	0	0	0

V. RESULTS

V. A. Calculated Results

V.A.1. Calculations of Emitted Decay Heat

As described in Sec. IV, nuclide concentrations and decay heat in each irradiated sample are cal-

[22] G. F. KUNCIR, "A Program for the Calculation of Resonance Integrals," GA-2525, General Atomics Division, General Dynamics Corporation (1961).

TABLE VIII

Calculated Percent of Gamma Rays in Each of Eight Energy Groups Captured in Each of Twenty Components of the System Comprising the ^{235}U-in-Al Sample, the Calorimeter, and the Canal

Component	Item[a]	Percent of Each Gamma-Ray Group Captured in Each Component							
		0	1	2	3	4	5	6	7
Fuel alloy	1	92.98	30.68	16.35	12.80	11.96	10.36	10.33	10.19
Cladding	1	6.12	9.50	5.87	4.48	4.18	2.77	2.90	3.16
Perforated basket	2(17)	0.30	1.87	1.74	1.09	1.37	1.15	1.17	1.11
Basket supports		0.00	0.39	0.27	0.35	0.33	0.06	0.15	0.30
Water inside		0.04	8.81	10.97	9.83	10.26	8.96	8.09	7.56
Stirrer and bushing	2(11,20)	0.00	0.83	0.64	0.37	0.41	0.34	0.42	0.32
Thermopile	2(12-14)	0.00	0.04	0.08	0.02	0.02	0.00	0.05	0.07
Brass of plug	3	0.00	0.10	0.11	0.08	0.05	0.01	0.02	0.11
Inner bottom	2	0.00	1.85	1.50	1.13	1.11	0.85	1.01	1.00
$\frac{1}{4}$-in.-thick inner cylinder	2(4)	0.50	11.78	10.16	8.13	7.40	6.76	5.97	5.20
$\frac{1}{16}$-in.-thick inner cylinder	2(4)	0.00	0.83	0.71	0.53	0.57	0.30	0.37	0.64
Nylon feed through	2(9)	0.00	0.01	0.03	0.05	0.05	0.06	0.01	0.02
All Teflon	2(7,15),3	0.06	1.35	1.83	2.16	1.84	1.56	1.31	0.88
Top + plug top	2(6,8)	0.00	1.46	1.81	1.70	1.71	1.72	1.75	1.74
Flange joining cylinders	2(21)	0.00	0.30	0.29	0.43	0.44	0.34	0.28	0.28
Vacuum space	2(1,2)	0.0	0.0	0.0	0.0	0.0	0.0	0.0	0.0
Outer cylinder	2(3)	0.00	5.57	5.15	4.84	3.81	4.01	3.96	3.80
Outer bottom	2	0.00	1.27	1.36	0.94	1.17	0.95	0.95	0.77
Water outside		0.00	18.77	30.70	34.36	33.92	35.35	34.31	33.01
Black absorber		0.00	4.59	10.43	16.71	19.40	24.45	26.95	29.84
Totals		100.00	100.00	100.00	100.00	100.00	100.00	100.00	100.00

[a]Each item is described in the figure listed. The number in parentheses designates the item in the figure.

culated in the COMBO procedure for each of 21 cooling times covering the range from 0.1 to 80 000 h. Although we normally calculate the total beta- and total gamma-ray heat at each cooling time, auxiliary cases studied by changing particular parameters permit distinguishing the heat due to various causes. In particular, the heat attributed to different nuclides or different types of decay can be distinguished and the importance of particular contributors can be assessed. This is shown in Figs. 7 through 10 where the heat calculated for the isotopic compositions in irradiated samples of ^{235}U, ^{233}U, ^{239}Pu, and ^{232}Th are graphed as functions of cooling time.

In Figs. 7 through 10, the heat indicated for ^{97}Nb includes that associated with the metastable state ^{97m}Nb. The heat indicated for the zirconium and niobium isotopes is that associated with activated structural nuclides in the cladding and alloy rods and does not include the fission-product heat due to such nuclides. The latter heat is properly included with the fission-product heat.

For cooling times less than 10 h, fission-product calculations using the COMBO procedure are incomplete because there are important short-lived nuclides not included among the 190 fission products currently considered.[12]

For the four fuels examined, the relative importance of the heat associated with fission products, heavy isotopes, and structural nuclides varies among the samples. Although fission-product heat is most important in the fissile materials, it is interesting to note the importance of heavy-isotope heat in ^{232}Th and ^{239}Pu.

The total heats from all the contributors in Figs. 7 through 10 are presented in column 2 of Tables IX through XII, respectively, for the cooling times of column 1. Column 3 presents the total charged particle heat due to beta and alpha particles plus conversion electrons, and column 4 gives the heat associated with gamma rays *per se*. The heat due to alpha particles or conversion electrons is <1% of the total except for two important cases. Alpha-particle decay is especially significant in irradiated plutonium at longer cooling times as shown in column 3a of Table XI where the part of the calculated charged-particle heat due to alpha particles is given. For irradi-

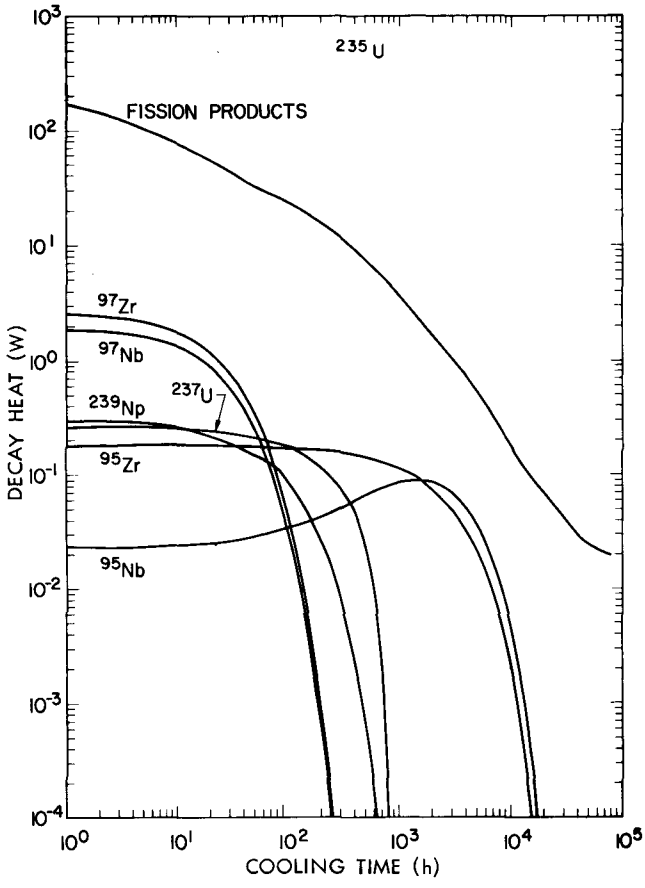

Fig. 7. Calculated decay heat in irradiated ^{235}U as a function of cooling time showing contributions by fission products, activated structural nuclides, and heavy isotopes.

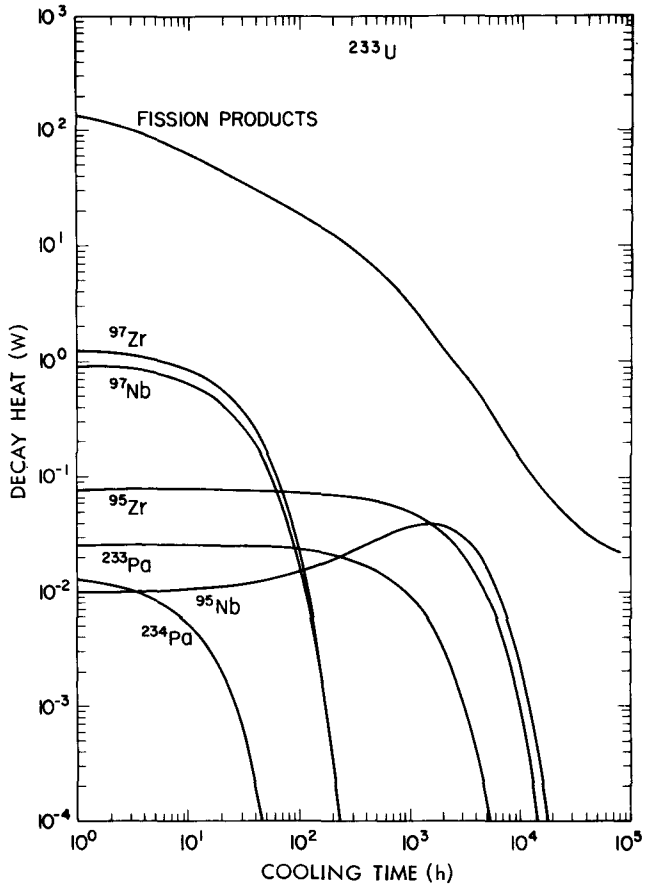

Fig. 8. Calculated decay heat in irradiated ^{233}U as a function of cooling time showing contributions by fission products, cladding nuclides, and heavy isotopes.

ated ^{232}Th, the importance of internal conversion is substantial as is evident in column 3a of Table XII where the part of the calculated charged-particle heat due to conversion electrons is given. Similar behavior would be expected for ^{238}U, although that fuel was not included in this program. In Table XII, the total heat due to gamma-ray transitions is given by the sum of columns 3a and 4.

V.A.2. Calculated Heat Captured in Calorimeter

The gamma-ray heat given in column 4 of Tables IX through XII is the sum of the heat due to gamma rays (excluding conversion electrons) calculated for the fission products, for heavy isotopes, and for structural activation products. Such gamma-ray heat is distributed in energy groups in the percentages shown in Tables V through VII for the heavy isotopes, fission products, and structural nuclides, respectively. The gamma-ray heat in each energy group is then absorbed in the 20 components according to the percentages given in Table VIII for ^{235}U. (Similar tabulations for the other three samples are not reproduced here.) For any cooling time, therefore, the gamma-ray heat in watts in a given irradiated sample is distributed among the 20 components in a readily calculable manner. Typical results of such calculations are given in Table XIII for the irradiated ^{235}U sample at 10 h cooling time. Here the calculated gamma-ray heat in each energy group is distributed over the 20 components as shown. Table XIII is typical of the results of calculations that have been carried out for each of the 21 cooling times and for each of the 4 irradiated samples. The horizontal sums in the right column of Table XIII give the total calculated heat from gamma rays absorbed in each component for 10 h of cooling time.

In Table XIII, as in Table VIII, the data are arranged from top to bottom in three different groups. From heat transfer considerations, the top group contains ten components whose absorbed gamma-ray heat is inside the calorimeter. Gamma-ray energy deposited in any of the seven com-

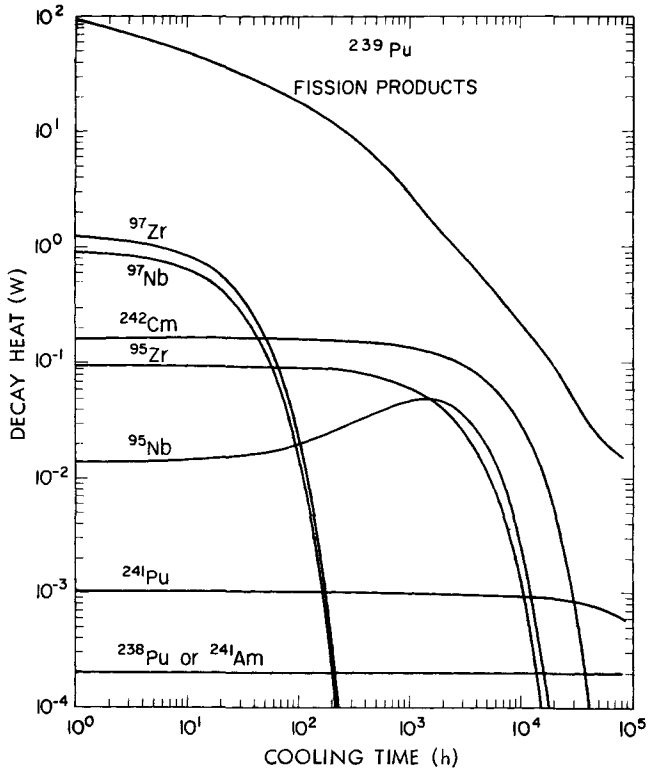

Fig. 9. Calculated decay heat in irradiated ^{239}Pu as a function of cooling time showing contributions by fission products, heavy isotopes, and cladding nuclides.

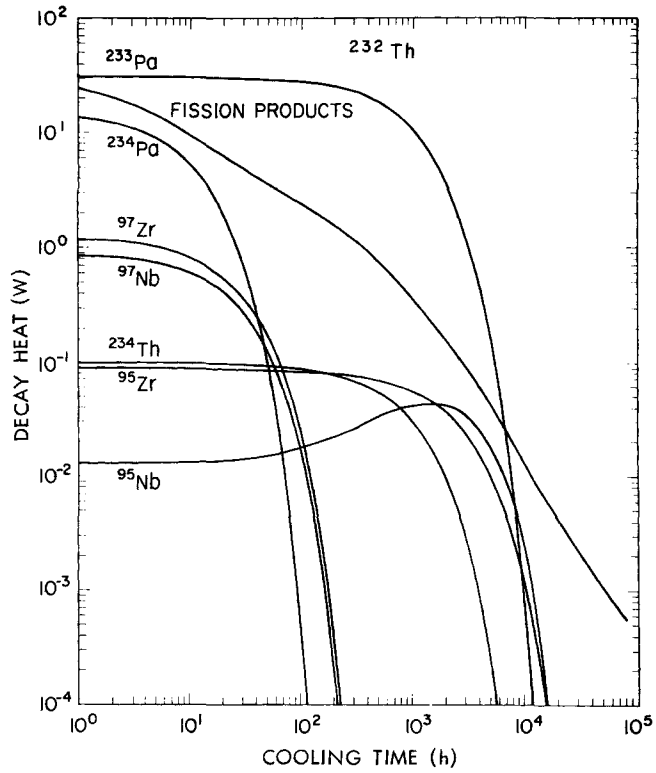

Fig. 10. Calculated decay heat in irradiated ^{232}Th as a function of cooling time showing contributions by heavy isotopes, fission products, and cladding nuclides.

TABLE IX

Calculated Decay Heat in Irradiated ^{235}U Sample That Escapes from or Is Captured in the Calorimeter

(1)	(2)	(3)	(4)	(4a)	(5)	(6)	(7)	(8)
Cooling Time (h)	Heat (W)					Percent Captured		Gamma-Ray % in 3 Components[a]
	Total	Total Charged Particle	Total Gamma Ray	Gamma-Ray Captured	Total Captured	Gamma-Ray	Total	
0.1	201.4	90.9	110.4	48.1	139.1	43.6	69.1	2.4
1	174.0	77.7	96.3	45.3	123.0	47.0	70.7	2.4
2	149.1	66.6	82.5	39.2	105.9	47.6	71.0	2.4
4	117.8	52.5	65.3	31.3	83.9	48.0	71.2	2.4
8	88.7	38.3	50.4	24.6	62.9	48.7	70.9	2.5
10	80.3	34.0	46.3	22.7	56.7	49.1	70.6	2.5
20	57.1	22.4	34.7	17.3	39.8	50.0	69.6	2.4
40	39.3	14.4	25.0	12.5	26.9	50.2	68.4	2.4
80	27.04	9.38	17.66	8.78	18.16	49.7	67.2	2.4
100	24.01	8.26	15.74	7.79	16.05	49.5	66.9	2.4
200	16.05	5.54	10.51	5.09	10.63	48.4	66.2	2.4
400	9.63	3.47	6.16	2.93	6.39	47.5	66.4	2.4
800	4.98	1.95	3.04	1.44	3.39	47.6	68.1	2.4
1 000	3.89	1.57	2.32	1.11	2.69	48.0	69.0	2.4
2 000	1.805	0.794	1.010	0.503	1.297	49.8	71.9	2.5
4 000	0.830	0.392	0.438	0.220	0.612	50.1	73.7	2.5
8 000	0.275	0.177	0.098	0.050	0.227	50.5	82.4	2.5
10 000	0.189	0.137	0.052	0.027	0.164	51.1	86.6	2.5
20 000	0.072	0.058	0.015	0.008	0.066	52.1	90.2	2.4
40 000	0.030	0.021	0.009	0.005	0.026	50.0	85.0	2.5
80 000	0.020	0.013	0.007	0.004	0.017	49.5	82.3	2.6

[a]The gamma-ray heat in these three components is produced partly inside and partly outside the calorimeter.

TABLE X

Calculated Decay Heat in Irradiated ^{233}U Sample That Escapes from or Is Captured in the Calorimeter

(1)	(2)	(3)	(4)	(4a)	(5)	(6)	(7)	(8)
Cooling Time (h)	Heat (W)					Percent Captured		Gamma-Ray % in 3 Components[a]
	Total	Total Charged Particle	Total Gamma Ray	Gamma-Ray Captured	Total Captured	Gamma-Ray	Total	
0.1	157.4	72.5	84.9	32.4	104.9	38.1	66.6	2.6
1	135.1	61.9	73.2	30.3	92.2	41.4	68.3	2.6
2	116.3	53.2	63.1	26.4	79.6	41.8	68.5	2.6
4	92.3	41.8	50.5	21.3	63.0	42.1	68.3	2.7
8	68.8	29.8	39.0	16.6	46.4	42.7	67.5	2.7
10	61.9	26.2	35.7	15.3	41.6	43.0	67.1	2.7
20	43.6	16.9	26.7	11.7	28.6	43.8	65.6	2.7
40	30.2	10.8	19.4	8.6	19.4	44.1	64.1	2.7
80	21.06	7.20	13.86	6.07	13.27	43.8	63.0	2.6
100	18.77	6.39	12.38	5.40	11.79	43.6	62.8	2.6
200	12.62	4.38	8.23	3.52	7.90	42.7	62.6	2.6
400	7.56	2.80	4.76	1.99	4.79	41.9	63.4	2.6
800	3.87	1.60	2.28	0.95	2.55	41.9	65.8	2.6
1 000	3.00	1.29	1.71	0.72	2.02	42.2	67.1	2.7
2 000	1.356	0.648	0.707	0.309	0.957	43.7	70.6	2.7
4 000	0.613	0.306	0.307	0.135	0.441	44.0	71.9	2.8
8 000	0.205	0.131	0.073	0.033	0.164	44.5	80.1	2.7
10 000	0.144	0.102	0.041	0.019	0.121	45.1	84.3	2.7
20 000	0.061	0.046	0.015	0.007	0.053	46.1	86.7	2.6
40 000	0.031	0.020	0.010	0.004	0.024	43.7	81.3	2.8
80 000	0.022	0.015	0.007	0.003	0.018	43.2	81.9	2.8

[a]See Table IX.

ponents of the bottom group is heat that is outside the calorimeter, and gamma-ray heat in the middle group is deposited partially inside the remainder outside the calorimeter. The three components in the middle group comprise the upper $\frac{1}{16}$-in.-thick part of the inner cylindrical can, the nylon feed-through shaft, and all the Teflon. Heat transfer considerations with the help of Curlee at the authors' Laboratory indicate that the small heat deposited in these three components is absorbed approximately two-thirds inside the calorimeter and one-third outside where these fractions have estimated uncertainties of one-sixth. When these proportions are applied to the sums given in the last column of Table XIII, the total heat from gamma rays absorbed inside the calorimeter is found to be 22.73 W while that outside the calorimeter is 23.60 W.

By similarly treating the data for all 21 cooling times of the ^{235}U sample, composite results calculated for the heat from gamma rays captured inside the calorimeter are obtained as presented in column 4a in Table IX. For the cooling times in column 1, the calculated heat from gamma rays escaping the calorimeter is the difference between columns 4 and 4a in Table IX. Column 5 gives the total calculated heat captured inside the calorimeter (columns 3 plus 4a). Column 6 gives the percent of the gamma-ray heat captured in the calorimeter and column 7 gives the percent of the total heat captured in the calorimeter. Column 8 gives the percent of the gamma-ray heat in the three components where the gamma rays are absorbed partially inside and partially outside the calorimeter. As can be seen in column 8, the total gamma-ray heat captured in the three components is small and essentially constant ($2.47 \pm 0.11\%$) over all cooling times, a situation that indicates these components are relatively unimportant and that the rough estimate of $\frac{2}{3} \pm \frac{1}{6}$ for the fraction of gamma-ray heat absorbed inside the calorimeter introduces an uncertainty of $<0.4\%$ in the calculated total power captured listed in column 5. Column 6 shows that the fraction of the gamma-ray power captured in the calorimeter is fairly constant; column 7 shows variations because the gamma-ray fraction of the total heat varies with cooling time.

Composite results of gamma-ray heat calculations derived from data such as those in Table XIII are used to complete columns 4a in Table IX for ^{235}U and in Tables X, XI, and XII for ^{233}U, ^{239}Pu, and ^{232}Th, respectively. The same sort of behavior is indicated for all four samples. Results in column 5 in each of Tables IX through XII give the total calculated heat captured inside the calorimeter. The column 5 results are plotted in Figs. 11 through 14 as smooth curves and represent the calculated results that are to be compared with the results of experimental measurements.

The calculation of the gamma-ray heat absorbed in the calorimeter is estimated to be accurate to about 5%, which contributes <2% to the uncertainty in the calculated total heat absorbed in the calorimeter. However, the total uncertainty in the calculations cannot be estimated at this time because it depends on various quantities (e.g., fission yields) that are common in calculations in the literature but whose accuracies are not established.

V. B. Measured Decay Heat Results

Experimental results of decay heat, obtained by the methods described in Sec. III, are given in Table XIV and shown as plotted points on Figs. 11 through 14 for ^{235}U, ^{233}U, ^{239}Pu, and ^{232}Th, respectively. These points on each figure compare

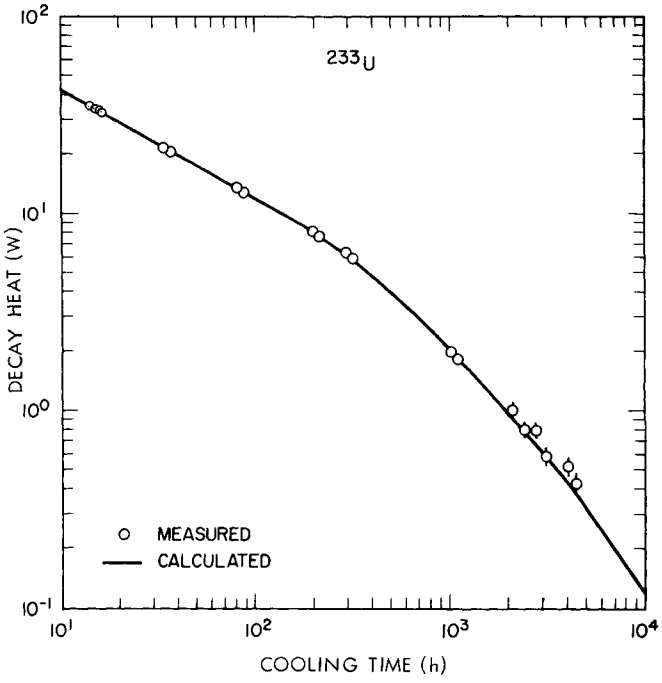

Fig. 12. Measured and calculated decay heat captured in calorimeter plotted as a function of cooling time for irradiated ^{233}U sample. Point size exceeds standard deviation except where indicated.

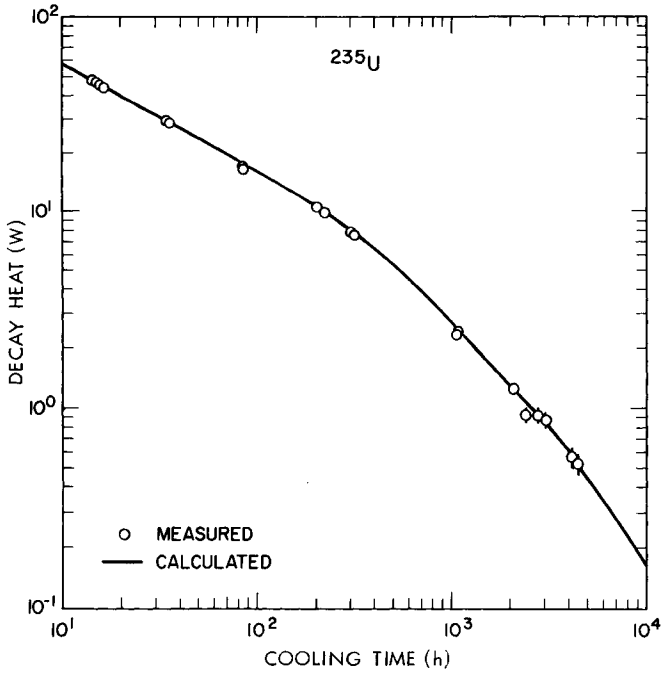

Fig. 11. Measured and calculated decay heat captured in calorimeter plotted as a function of cooling time for irradiated ^{235}U sample. Point size exceeds standard deviation except where indicated.

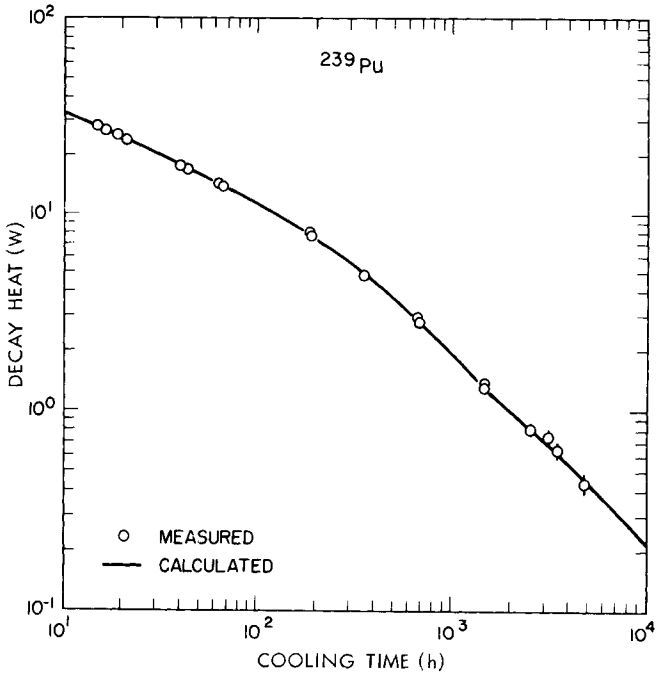

Fig. 13. Measured and calculated decay heat captured in calorimeter plotted as a function of cooling time for irradiated ^{239}Pu sample. Point size exceeds standard deviation except where indicated.

TABLE XI

Calculated Decay Heat in Irradiated ^{239}Pu Sample That Escapes from or Is Captured in the Calorimeter

(1)	(2)	(3)	(3a)	(4)	(4a)	(5)	(6)	(7)	(8)
Cooling Time (h)	Heat (W)						Percent Captured		Gamma-Ray % in 3 Components[a]
	Total	Total Charged Particle	Alpha	Total Gamma Ray	Gamma-Ray Captured	Total Captured	Gamma-Ray	Total	
0.1	108.5	46.0	0.17	62.5	23.8	69.8	38.1	64.4	2.6
1	94.4	39.4	0.17	55.0	22.8	62.2	41.4	65.9	2.6
2	82.5	34.2	0.17	48.2	20.2	54.4	41.9	66.0	2.6
4	67.8	27.8	0.17	40.1	16.9	44.6	42.1	65.8	2.7
8	54.2	21.5	0.17	32.8	14.0	35.4	42.7	65.3	2.7
10	50.2	19.5	0.17	30.6	13.2	32.7	43.0	65.2	2.7
20	38.3	14.1	0.17	24.2	10.6	24.7	43.8	64.5	2.7
40	28.2	9.8	0.17	18.4	8.1	17.9	44.1	63.6	2.7
80	20.23	6.75	0.16	13.48	5.90	12.65	43.8	62.5	2.6
100	18.07	5.98	0.16	12.09	5.27	11.25	43.6	62.3	2.6
200	12.13	4.03	0.16	8.10	3.46	7.49	42.7	61.7	2.6
400	7.28	2.53	0.15	4.75	1.99	4.51	41.9	62.0	2.6
800	3.79	1.45	0.14	2.34	0.98	2.43	41.8	64.1	2.6
1 000	2.98	1.19	0.14	1.78	0.75	1.95	42.2	65.3	2.7
2 000	1.43	0.68	0.12	0.75	0.33	1.01	43.7	70.5	2.7
4 000	0.732	0.421	0.082	0.311	0.137	0.558	43.9	76.2	2.8
8 000	0.322	0.241	0.041	0.081	0.036	0.277	44.4	86.0	2.7
10 000	0.244	0.194	0.029	0.050	0.023	0.217	45.1	88.8	2.7
20 000	0.097	0.078	0.006	0.019	0.009	0.087	46.1	89.4	2.6
40 000	0.032	0.021	0.001	0.011	0.005	0.026	43.8	80.7	2.8
80 000	0.017	0.100	0.001	0.007	0.003	0.013	43.2	76.6	2.8

[a]See Table IX.

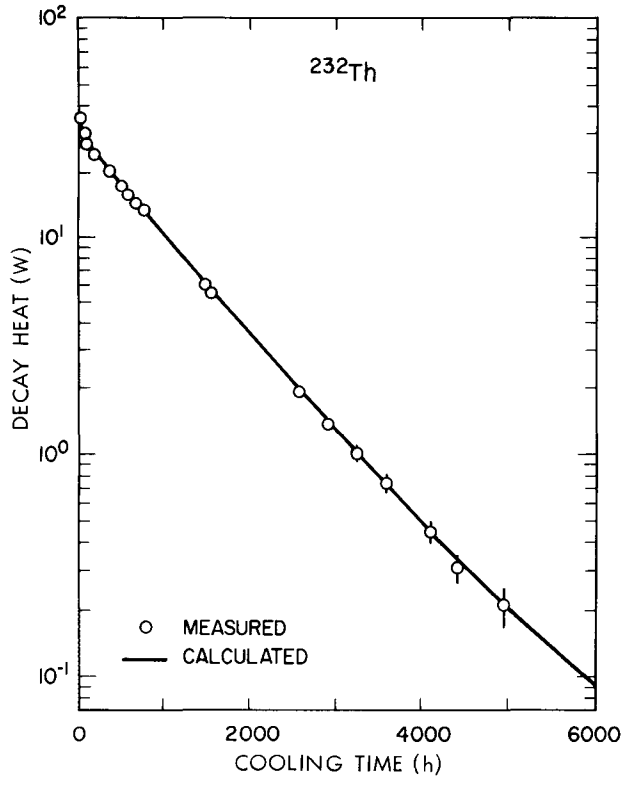

Fig. 14. Measured and calculated decay heat captured in calorimeter plotted as a function of cooling time for irradiated ^{232}Th sample. Point size exceeds standard deviation except where indicated.

directly with the curve calculated for the heat captured within the calorimeter. By running additional COMBO problems for the specific cooling times of the experimental measurements as given in Table XIV, calculated results for the total captured heat at the time of each measurement have also been obtained and are included in Table XIV. Comparing measurement with calculation for all the data above 2.5 W shows rms deviations of only ±3.3, ±2.4, ±1.9, and ±2.4% for ^{235}U, ^{233}U, ^{239}Pu, and ^{232}Th, respectively. This comparison includes 60 to 75% of the measurement data, but excludes lower power data because of larger measurement uncertainties as given in Table II.

V. C. Uranium-235 Measurements Compared with Calculations Per Proposed ANS Standard ANS-5.1

In October 1971, the American Nuclear Society issued a Draft Standard ANS-5.1 (ANSI N18.6)

TABLE XII

Calculated Decay Heat in Irradiated ^{232}Th Sample That Escapes from or Is Captured in the Calorimeter

(1)	(2)	(3)	(3a)	(4)	(4a)	(5)	(6)	(7)	(8)
Cooling Time (h)	Heat (W)						Percent Captured		Gamma-Ray % in 3 Components[a]
	Total	Total Charged Particle	Internal Conversion	Gamma Ray	Gamma-Ray Captured	Total Captured	Gamma-Ray	Total	
0.1	75.7	35.9	15.6	39.8	26.6	62.6	67.0	82.7	1.3
1	69.9	33.5	15.4	36.4	25.3	58.8	69.4	84.1	1.2
2	64.7	31.3	15.2	33.4	23.6	54.9	70.7	84.9	1.1
4	57.5	28.4	14.8	29.1	21.1	49.5	72.5	86.1	1.1
8	49.3	25.0	14.2	24.2	18.2	43.3	75.2	87.8	1.0
10	46.6	24.0	14.0	22.6	17.3	41.2	76.3	88.5	0.9
20	39.2	21.0	13.3	18.2	14.5	35.6	80.0	90.8	0.8
40	34.3	19.0	12.7	15.2	12.7	31.7	83.0	92.4	0.6
80	31.14	17.54	12.17	13.60	11.47	29.01	84.3	93.2	0.6
100	30.19	17.06	11.91	13.13	11.10	28.16	84.6	93.3	0.6
200	26.55	15.14	10.70	11.42	9.73	24.86	85.2	93.6	0.5
400	21.13	12.13	8.64	9.00	7.71	19.84	85.8	93.9	0.5
800	13.66	7.88	5.63	5.78	4.99	12.86	86.2	94.2	0.5
1 000	11.02	6.36	4.55	4.66	4.03	10.38	86.3	94.2	0.5
2 000	3.85	2.20	1.56	1.64	1.41	3.62	86.0	94.0	0.5
4 000	0.525	0.285	0.183	0.240	0.197	0.482	82.1	91.8	0.7
8 000	0.032	0.017	0.003	0.015	0.010	0.027	69.5	85.7	1.3
10 000	0.016	0.010	0.000	0.006	0.004	0.014	67.2	87.7	1.4
20 000	0.005	0.004	0.000	0.001	0.001	0.005	67.0	93.4	1.4
40 000	0.001	0.001	0.000	0.000	0.000	0.001	---	---	---
80 000	0.001	0.001	0.000	0.000	0.000	0.001	---	---	---

[a] See Table IX.

TABLE XIII

Calculated Gamma-Ray Heat in Irradiated ^{235}U Sample After 10 h Cooling Time

Component	Power Deposited in Each Energy Group and in Each Component (W)								
	0	1	2	3	4	5	6	7	Total
Fuel alloy	0.73	1.83	4.11	0.62	0.89	0.10	0.08	0.04	8.40
Cladding	0.05	0.57	1.48	0.22	0.31	0.03	0.02	0.01	2.68
Perforated basket	0.00	0.11	0.44	0.05	0.10	0.01	0.01	0.00	0.73
Basket supports	0.00	0.02	0.07	0.02	0.02	0.00	0.00	0.00	0.14
Water inside	0.00	0.53	2.76	0.47	0.76	0.09	0.06	0.03	4.70
Stirrer and bushing	0.00	0.05	0.16	0.02	0.03	0.00	0.00	0.00	0.27
Thermopile	0.00	0.00	0.02	0.00	0.00	0.00	0.00	0.00	0.03
Brass of plug	0.00	0.01	0.03	0.00	0.00	0.00	0.00	0.00	0.04
Inner bottom	0.00	0.11	0.38	0.05	0.08	0.01	0.01	0.00	0.64
$\frac{1}{4}$-in. thick inner cylinder	0.00	0.70	2.56	0.39	0.55	0.07	0.05	0.02	4.34
$\frac{1}{16}$-in.-thick inner cylinder	0.00	0.05	0.18	0.03	0.04	0.00	0.00	0.00	0.31
Nylon feed through	0.00	0.00	0.01	0.00	0.00	0.00	0.00	0.00	0.02
All Teflon	0.00	0.08	0.46	0.10	0.14	0.02	0.01	0.00	0.81
Top + plug top	0.00	0.09	0.45	0.08	0.13	0.02	0.01	0.01	0.79
Flange joining cylinders	0.00	0.02	0.07	0.02	0.03	0.00	0.00	0.00	0.15
Vacuum space	0.00	0.00	0.00	0.00	0.00	0.00	0.00	0.00	0.00
Outer cylinder	0.00	0.33	1.30	0.23	0.28	0.04	0.03	0.01	2.23
Outer bottom	0.00	0.08	0.34	0.05	0.09	0.01	0.01	0.00	0.57
Water outside	0.00	1.12	7.72	1.66	2.53	0.35	0.26	0.13	13.77
Black absorber	0.00	0.27	2.62	0.81	1.44	0.24	0.21	0.11	5.71
Totals	0.78	5.98	25.15	4.82	4.45	1.00	0.77	0.38	46.33

TABLE XIV

Measured and Calculated Decay Heat as a Function of Cooling Time for ^{235}U, ^{233}U, ^{239}Pu, and ^{232}Th

^{235}U Sample 25			^{233}U Sample 45			^{239}Pu Sample 19			^{232}Th Sample 41		
Cooling Time (h)	Decay Heat (W)		Cooling Time (h)	Decay Heat (W)		Cooling Time (h)	Decay Heat (W)		Cooling Time (h)	Decay Heat (W)	
	Meas	Calc		Meas	Calc		Meas	Calc		Meas	Calc
14.55	46.9	47.1	14.12	35.0	34.7	14.83	28.6	28.0	14.42	35.8	37.9
14.97	46.3	46.4	14.77	35.2	33.8	15.57	27.5	27.5	18.38	35.4	36.2
15.45	45.3	45.7	15.67	34.0	32.7	18.57	25.9	25.5	41.23	30.7	31.5
15.90	44.5	45.0	16.14	33.2	32.2	20.80	24.1	24.3	41.80	31.0	31.5
34.49	29.09	29.29	34.17	21.70	21.17	40.55	17.69	17.80	65.07	29.15	29.76
35.49	28.82	28.82	35.25	20.99	20.80	42.03	17.73	17.49	66.40	28.84	29.69
81.77	17.57	17.95	81.47	13.38	13.15	64.73	14.14	14.10	185.6	24.71	25.29
83.34	16.81	17.76	83.07	13.11	13.01	65.33	14.15	14.03	186.0	24.79	25.27
201.5	10.55	10.58	201.2	7.80	7.87	185.3	8.04	7.87	353.7	20.57	20.89
202.2	10.31	10.56	201.7	7.94	7.86	185.8	7.82	7.85	354.2	20.70	20.87
296.3	7.57	8.08	296.8	6.26	6.03	353.9	4.88	4.97	499.9	17.56	17.79
297.6	7.55	8.05	297.0	6.04	6.02	665.9	2.95	2.90	501.1	17.59	17.76
1067	2.36	2.51	1069	1.90	1.87	668.6	3.04	2.89	547.5	16.58	16.89
1068	2.44	2.50	1069	1.97	1.87	1510	1.30	1.30	549.0	16.29	16.86
2099	1.23	1.24	2100	1.02	0.91	1511	1.37	1.30	665.6	14.42	14.86
2436	0.93	1.06	2435	0.80	0.78	2563	0.82	0.82	668.4	14.51	14.82
2770	0.92	0.93	2772	0.78	0.68	3234	0.75	0.67	762.5	13.47	13.39
3108	0.88	0.82	3105	0.58	0.60	3572	0.65	0.62	762.6	13.29	13.39
4142	0.56	0.59	4139	0.52	0.42	4919	0.44	0.46	1511	6.21	6.04
4451	0.52	0.53	4450	0.43	0.38				1511	5.96	6.04
									2565	1.92	2.01
									2899	1.36	1.43
									3235	1.01	1.02
									3571	0.74	0.73
									4075	0.45	0.45
									4385	0.31	0.34
									4918	0.21	0.21

entitled "Decay Energy Release Rates Following Shutdown of Uranium-Fueled Thermal Reactors." The Standard provides an estimate of decay heat in arbitrary mixtures of ^{235}U and ^{238}U, irradiated either for an infinite or for a finite period of time at constant power, and then instantaneously shut down. Since the Standard applies to irradiated ^{235}U, it would be worthwhile to check the Standard by comparing calculations obtained using the Standard with the measured decay heat in the irradiated ^{235}U sample. Although heavy-isotope heat in ^{239}Np is included as a part of the Standard, the interest here is directed toward the more important fission-product heat.

For cooling times of interest after the first 10^3 sec following shutdown, the Standard is based on the work of Perkins and King[8] as modified by Perkins (see discussion in Ref. 2) and as described by Shure.[17] It is based on the decay heat of 123 fission products and includes coupling by beta-particle or gamma-ray decay, but makes no provisions for capture coupling or fission-product depletion.

Strictly speaking, the Standard pertains to a single-step irradiation at constant power. In contrast, the ^{235}U sample was irradiated for three exposure cycles in the MTR followed a year or so later by a more intense exposure for one cycle in the ATR. As shown in Ref. 13, the exposure history for the ^{235}U sample is described by a sequence of 230 different steps in 3 energy groups, where the fission rates are treated as constant during any step but vary from step to step. There is no way to approximate a real exposure history meaningfully by a single step at constant power. Instead, the Standard can be applied to each power step in turn and the results summed to obtain the total heat calculated by the Standard for the real exposure history.

To carry out this procedure, the provision in

the Standard for a single-step irradiation at constant power has been extended by Shure and Wallace in the so-called FSTAB procedure[2] to accommodate a sequence of steps and, therefore, a real exposure history. The application of the FSTAB procedure to the real exposure history of the irradiated ^{235}U sample provides the calculated fission-product decay heat consistent with what the Standard would give if it were applied step-by-step to the real history, with the results from each step summed to obtain the total effect. The results of the FSTAB problem are considered to be the Standard results and are based on the same basic data as the Standard. These so-called Standard results are plotted as the smooth curve in Fig. 15.

Since the Standard is not applicable to irradiated ^{233}U, ^{239}Pu, or ^{232}Th, calculations based on the Standard are presented only for the irradiated ^{235}U case.

To compare the Standard curve of Fig. 15 with experimental results, the experimental data were adjusted upward to include the gamma-ray energy calculated to escape from the calorimeter, and then the calculated heat due to heavy isotopes and structural nuclides was subtracted to get the total fission-product heat indicated by the measurements. The procedure is illustrated in Table XV where the first two columns give the cooling time and decay heat for the ^{235}U sample measured in the calorimeter. For each of the cooling times shown, the fraction of the total calculated heat captured in the calorimeter is interpolated from a graph of the data of column 7 in Table IX and is given in column 3 of Table XV. The quotient obtained by dividing the results in column 2 of Table XV by those in column 3 gives the total heat indicated by the measurements and given in column 4. The sum of the calculated heat associated with heavy isotopes and structural nuclides is obtained from Fig. 7 and a graph of such data is interpolated to obtain the results tabulated in column 5 for each of the cooling times of column 1. By subtracting column 5 from column 4, the results in column 6 are obtained for the total fission-product heat indicated by the measurements. The results in column 6 are plotted as experimental points in Fig. 15 where comparison with the curve for the Standard indicates very good agreement.

For each measured cooling time in column 1 of Table XV, the calculated heating obtained from the Standard is tabulated in column 7. Columns 6 and 7 show how the measured fission-product heat and that calculated using the Standard compare.

TABLE XV

Comparison of Irradiated ^{235}U Fission-Product Heat Derived from Experimental Measurements and Calculated from Standard ANS-5.1

(1)	(2)	(3)	(4)	(5)	(6)	(7)
Cooling Time (h)	Measured Captured Heat (W)	Calculated Ratio of Captured to Total Heat	"Measured" Total Heat (W)	Calculated Heavy-Isotope + Structural Heat (W)	"Measured" Fission-Product Heat (W)	Calculated ANS-5.1 Std Fission-Product Heat (W)
14.55	46.9	0.7015	66.9	1.8	65.1	63.8
14.97	46.3	0.7005	66.1	1.7	64.4	62.9
15.45	45.3	0.7000	64.7	1.7	63.0	61.8
15.90	44.5	0.6998	63.6	1.7	61.9	60.9
34.49	29.09	0.6860	42.41	0.92	41.49	39.99
35.49	28.82	0.6855	42.04	0.89	41.15	39.36
81.77	17.57	0.6715	26.17	0.34	25.83	25.30
83.34	16.81	0.6710	25.05	0.33	24.72	25.04
201.49	10.55	0.6620	15.94	0.21	15.73	15.12
202.17	10.31	0.6620	15.57	0.21	15.36	15.09
296.30	7.57	0.6620	11.44	0.20	11.24	11.51
297.57	7.55	0.6620	11.40	0.20	11.20	11.48
1067	2.36	0.6925	3.41	0.18	3.23	3.35
1068	2.44	0.6925	3.52	0.17	3.35	3.35
2099	1.23	0.7198	1.71	0.14	1.57	1.55
2436	0.93	0.7230	1.29	0.13	1.16	1.32
2770	0.92	0.7252	1.27	0.12	1.15	1.15
3108	0.88	0.7277	1.21	0.11	1.10	1.01
4142	0.56	0.7390	0.76	0.07	0.69	0.71
4451	0.52	0.7430	0.70	0.06	0.64	0.64

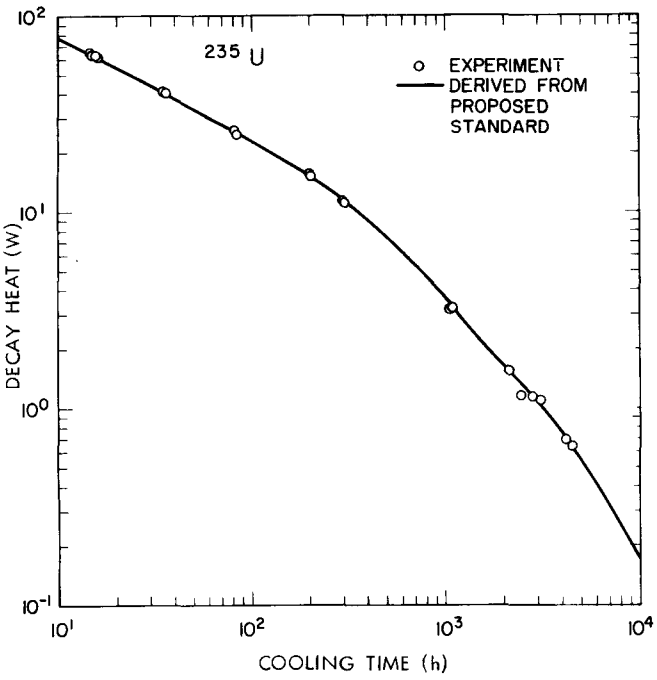

Fig. 15. Comparison of irradiated ^{235}U fission-product heat obtained from experimental measurements and calculated from the Proposed Standard ANS-5.1 by summing results obtained for all flux steps.

For all the data above 2.5 W, the more accurate data per Table II, the comparison of measurement with calculation shows an rms deviation of only ±2.7%.

VI. DISCUSSION

As illustrated in the calculational results in Figs. 7 through 10, nonfuel activation products of the zirconium cladding and alloy contribute significantly to the decay heat in all the irradiated fuel samples used in these experiments—from $2\frac{1}{2}$ to 4% for cooling times in the neighborhood of 10 h and from 5 to 20% for cooling times of several thousand hours. Heat associated with the decay of heavy isotopes is the major contributor in irradiated fertile fuel (natural ThO_2) for cooling times to 7000 h; and the heat associated with the alpha-particle decay of ^{242}Cm contributes more than 14% of the total heat in irradiated ^{239}Pu at several thousand hours cooling time. The heat due to ^{242}Cm is important for decay-heat considerations in irradiated natural uranium or plutonium and has potential importance for the fast breeder reactor.

In calorimetric measurements of irradiated fuels, where some of the gamma-ray decay energy escapes the calorimeter, calculations of the heat captured in the calorimeter must account explicitly for the absorption of the gamma-transition energy carried by conversion electrons. This is particularly true for irradiated thorium.

The shape of the gamma-ray spectrum computed for fission products, as described in Sec. IV. B. 2 and given in Table VI, pertains only to the ^{235}U sample and to its irradiation history. For want of other information, this ^{235}U spectral shape has been used for the fission-product gamma rays in all four of the irradiated fuel samples. In view of the agreement between measurement and calculation of decay heat as shown in Figs. 11 through 14 and in Table XIV, there is no evidence that use of the fission-product spectral shape calculated for the irradiated ^{235}U sample has introduced difficulties in the calculated results for the other three samples.

In the results presented in this report, decay heat is expressed in power units (watts) rather than as a ratio of decay-to-fission power as is the case in the Proposed Standard ANS-5.1 and in a number of the references. Although use of the power ratio can be instructive for design calculations, it is not appropriate for cases involving real exposures with variable operating power.

As written, the Proposed Standard ANS-5.1 is intended to provide an estimate of decay heat in ^{235}U and ^{238}U fueled reactors. For the cases of these experiments, the Standard is reportedly reliable within +10 and -20% for cooling times from 14 to 2800 h, and within +25 and -50% for longer cooling times. In view of the fission-product decay-heat results presented in Fig. 15 and Table XV, the uncertainties assigned in the Standard appear to be very conservative, a comforting situation for a standard. Whether such conservatism would exist for fuel of other ^{235}U enrichments, for shorter or longer cooling times, or for irradiation exposures substantially different from those of the present ^{235}U experiment has not been established.

Of perhaps greater long-range importance than the ^{235}U and Standard comparison are the agreements between measurement and detailed calculation shown in Figs. 11 through 14 and in Table XIV for the four fuels. Since these agreements are found for four different fuels, the confidence in our ability to calculate decay heat in more general situations is enhanced. Because the agreements described are closer than either calculational or experimental uncertainties would predict, it is evident that we have either overestimated uncertainties or that some systematic effects have fortuitously cancelled. Comparisons of measurement and calculation of decay heat for all samples and cooling times indicate agreement within two standard deviations (of the measured heat cap-

tured within the calorimeter). For cooling times less than 1000 h, the agreement is generally within 2%.

VII. CONCLUSIONS

Measurements of decay heat in irradiated ^{235}U, ^{233}U, ^{239}Pu, and ^{232}Th have been carried out for cooling times from 14 to 4500 h. Corresponding calculations based on the measured detailed exposure history show remarkable agreement with the measurements, generally within about 2%. Calculations according to the Proposed Standard ANS-5.1 for the case of irradiated ^{235}U agree with measurements within a few percent, which is much better than expected in view of the uncertainties in the Standard.

ACKNOWLEDGMENTS

The authors are grateful to E. I. Markiewicz for fabricating calorimeter components and other items of equipment; to L. L. Wheat for making arrangements at the irradiation facility for irradiations and measurements; to the staff of the Advanced Reactivity Measurement Facility for carrying out calorimetric measurements; to H. D. Cook, C. J. Rettger, W. E. George, and F. B. Barker for mass spectrometric and radiochemical analyses; to R. D. Wills for flux-monitor activation counting; to N. R. Candelore and G. Tessler for assistance in Monte Carlo calculations of gamma-ray escape probabilities; to J. P. Nelis and W. J. Petras for data processing; and to Deborah A. Iannuzzi for programmatic and computational assistance.

This work was carried out under the auspices of the U.S. Atomic Energy Commission, Contract AT(36-1)-GEN-14.